Implementation of All-sky Microwave Radiance Assimilation in JMA's Global NWP System

SHIMIZU Hiroyuki, KAZUMORI Masahiro and KADOWAKI Takashi
Numerical Prediction Division, Japan Meteorological Agency

1. Introduction

Data from space-based microwave radiance observation contains a variety of information on geophysical parameters relating to the atmosphere and the earth's surface (e.g., atmospheric temperature, water vapor, cloud, precipitation, surface wind and surface temperature). In this context, microwave radiance over ocean areas in clear-sky conditions has been assimilated in JMA's global numerical weather prediction (NWP) system since May 2003 (Okamoto et al. 2005). As data on microwave radiance from cloud and precipitation contain information on the presence of water/ice particles, assimilation of all-sky (including clear-sky, cloud and precipitation) microwave radiance contributes to better forecasting of atmospheric phenomena associated with severe weather conditions. The tracing effect of such assimilation based on 4D-Var also helps to improve dynamic initial conditions and supports improved forecasting (Geer et al. 2014).

JMA developed all-sky microwave assimilation scheme for microwave water-vapor sounders and microwave imagers (Kazumori and Kadowaki 2017) including outer-loop iteration for trajectory updates in the 4D-Var minimization process for effective assimilation of cloud and precipitation data. The scheme was introduced into JMA's operational global NWP system in December 2019.

This report gives an overview of the all-sky assimilation scheme and its impact on analysis, regular forecasting and tropical cyclone (TC) forecasting. Section 2 outlines the all-sky assimilation scheme, Section 3 details impacts on analysis, regular forecasting and TC forecasting, and Section 4 provides a summary.

2. Data and Quality Control

The RTTOV-SCATT (Radiative Transfer for TOVS; Bauer et al. 2006) model enables multiple-scattering radiative transfer calculation for microwave frequencies as part of the RTTOV-10 package, and is adopted as an observation operator for all-sky assimilation processing. Observation error assignment based on the symmetric (the average of observation and first guess (FG)) cloud amount (Geer and Bauer 2011) is used because cloud-influenced observation error has non-Gaussian distribution. Biased data caused by insufficient cloud representation in JMA's global forecast model (e.g., cold-sector bias) are removed. The all-sky assimilation scheme is applied to microwave water-vapor sounder (GMI/GPM, MHS/NOAA-19, Metop-A, -B) and microwave imager (AMSR2/GCOM-W, GMI/GPM, SSMIS/DMSP F-17, F-18), assimilated in clear-sky condition before. Furthermore, two additional microwave sensors (WindSat/Coriolis, MWRI/FY-3C) which have not been utilized in JMA's global NWP system are included in the all-sky assimilation sensors.

Figure 1 shows microwave imager data coverage in the data assimilation time window for 00 UTC on 1 December 2019, indicating an expansion after the implementation of all-sky microwave radiance assimilation. The number of data used increased by a factor of around five as a result of the all-sky assimilation and the addition of new sensor data.

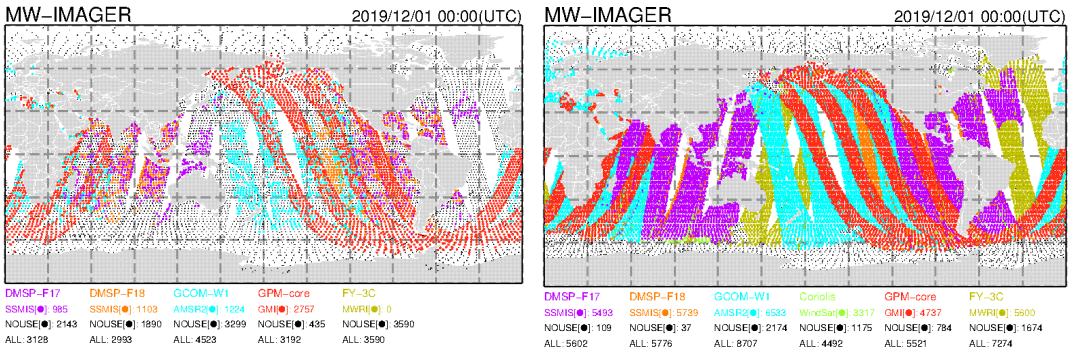

Figure 1. Microwave imager data coverage in the data assimilation time window for 00 UTC on 1 December 2019. Left: before implementation of the all-sky assimilation scheme; right: after.

3. Impact Evaluation: Data Assimilation Experiments

(a) Experiment configuration

Data assimilation experiments were conducted using JMA's global NWP system for the period from November 2017 to March 2018 (winter 2018) and June to October 2018 (summer 2018). The CNTL experiment had the same configuration as JMA's operational global NWP system for December 2018, and TEST experiment had the all-sky assimilation scheme of microwave water-vapor sounders (GMI/GPM, MHS/NOAA-19, Metop-A, -B) and microwave imagers (AMSR2/GCOM-W, GMI/GPM, SSMIS/DMSP F-17, F-18, WindSat/Coriolis, MWRI/FY-3C) with outer-loop iteration (twice) for trajectory updates in the 4D-Var minimization process.

(b) Impacts on analysis and forecast fields

Figure 2 shows differences in the standard deviations of SAPHIR (183.31±11 GHz) FG departure statistics and the number of used data, which are sensitive to lower tropospheric water vapor. SAPHIR data were assimilated under clear-sky conditions for both experiments. The number of data in TEST was higher and the standard deviations for FG departure were lower, indicating improved FG water vapor fields for the lower troposphere in the tropics. FG data matched other observation information such as surface wind speed from scatterometers and AMSU-A radiance data (channel 4, 52.8 GHz, which is sensitive to lower tropospheric temperature). These results indicate improved lower tropospheric wind and temperature fields in FG (Figure 3).

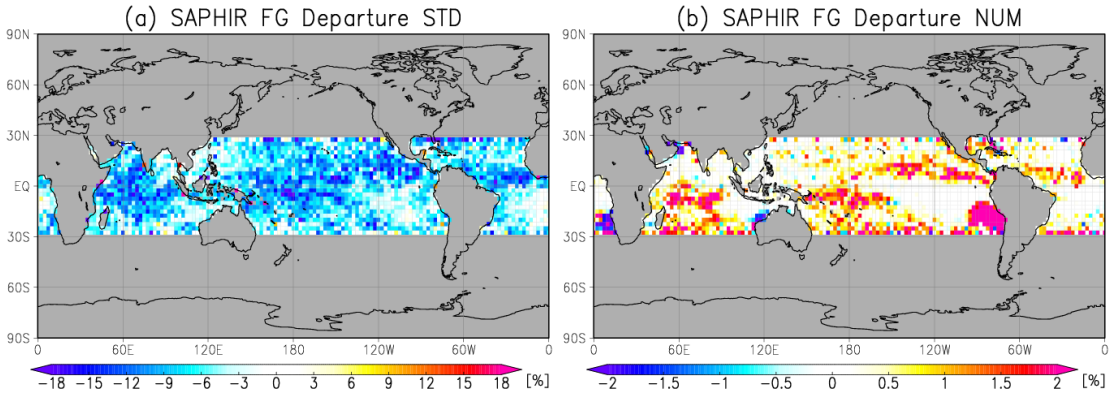

Figure 2. (a) Normalized changes for SAPHIR (183.31±11 GHz) standard deviations of FG departures and (b) ratio of number of data used (%)

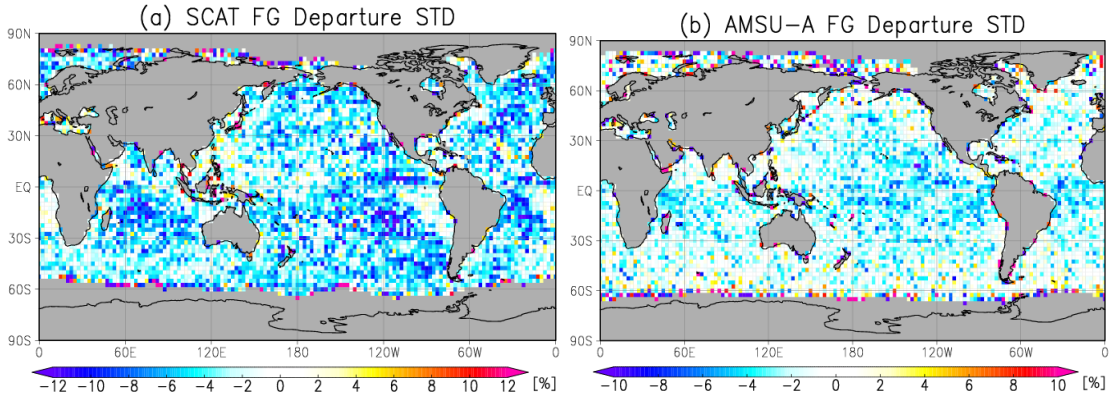

Figure 3. Normalized changes in standard deviations of FG departure for (a) scatterometer (ASCAT) wind speed and (b) AMSU-A at 52.8 GHz radiance

Figure 4 shows the improvement ratio for the root mean square error (RMSE) of geopotential height at 500 hPa verified against own analyses. The RMSE improved for the whole forecast range to 96 hours in the summer and winter experiments, and other elements (e.g., sea level pressure and wind speed at 850 hPa) also improved (not shown).

Figure 5 shows average TC track forecast errors and differences between TEST and CNTL for the summer and winter experiments. Errors in TEST decreased for the whole forecast range to 96 hours, and the decrease was statistically significant up to 72 hours.

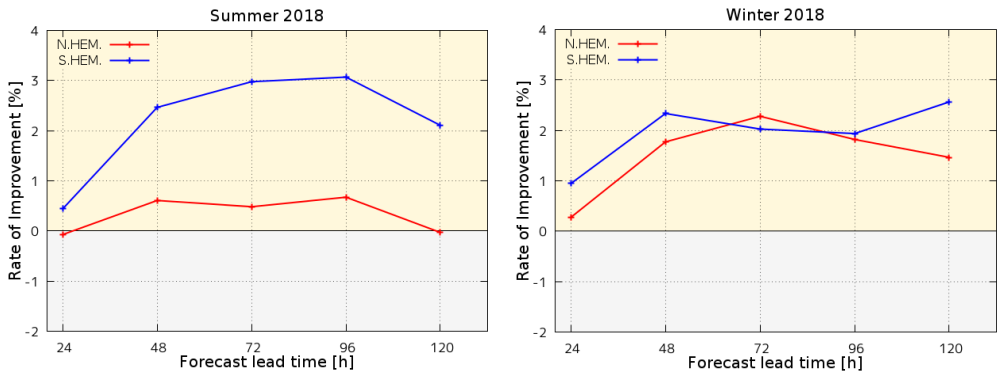

Figure 4. Improvement ratio ((CNTL – TEST) / CNTL) [%]) for the RMSE of geopotential height at 500 hPa verified against own analysis. Positive values indicate forecast error reductions of TEST against CNTL. The figures on the left and right show results for summer and winter 2018, respectively. Red and blue lines show verification results for the Northern Hemisphere (20 – 90°N) and the Southern Hemisphere (20 – 90°S), respectively.

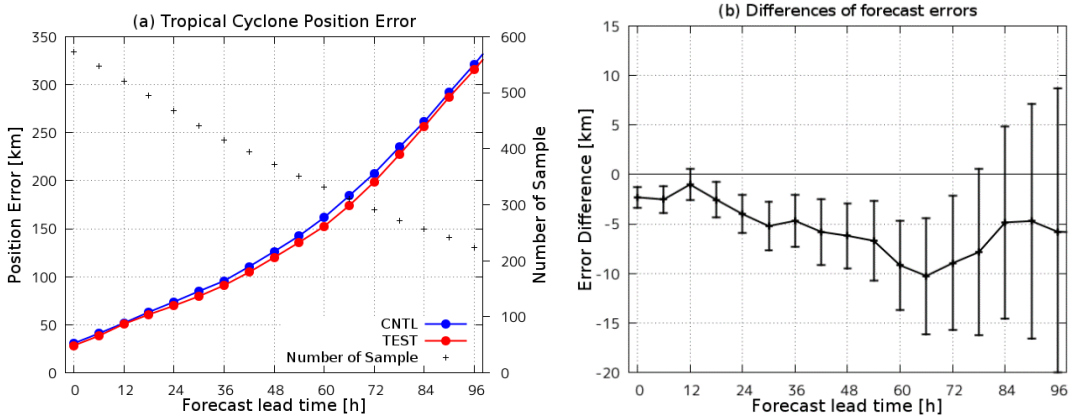

Figure 5. (a) Average TC track forecast errors for the summer and winter experiments. The red and blue lines are for TEST and CNTL, respectively, and dots represent sample data numbers. (b) Forecast error differences between TEST and CNTL. Error bars represent a 95% confidence interval.

(c) Case study (Typhoon Jebi (T1821))

Analysis of Typhoon Jebi (T1821; Figure 6) shows better TC track and intensity forecasting for TEST than for CNTL as of 06 UTC on 29 August 2018 with the initial conditions. In Figure 7, black dots show assimilated microwave imager data, colors show total column water vapor amounts, and contours show surface pressure fields. TEST show a microwave imager data distribution around the TC center, while most such data are screened out in CNTL. Higher water vapor values are seen in TEST as a result of microwave imager assimilation around the TC center. The temperature anomaly in the cross section at the TC center (Figure 8) indicates an enhanced warm-core structure in TEST. Improved water vapor fields around the TC center contributed to better TC track and intensity forecasting.

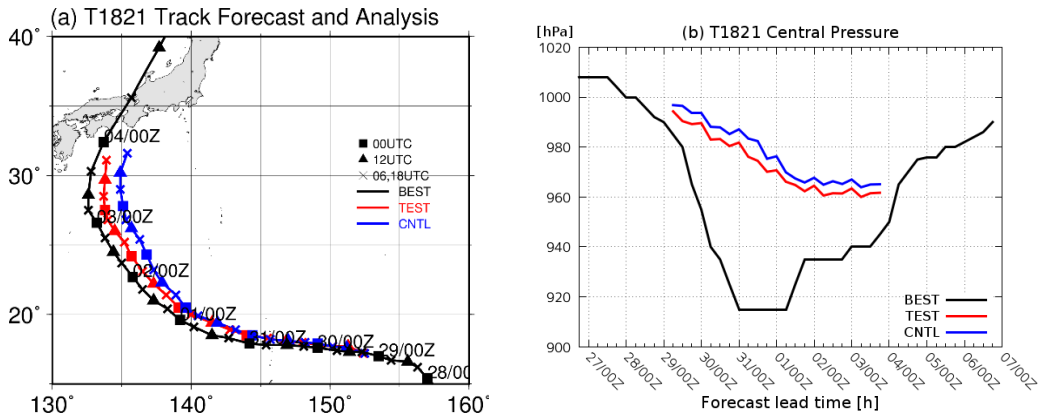

Figure 6. (a) TC track and (b) central pressure forecasts for Typhoon Jebi. The black, red and blue lines represent the JMA best track, TEST and CNTL, respectively.

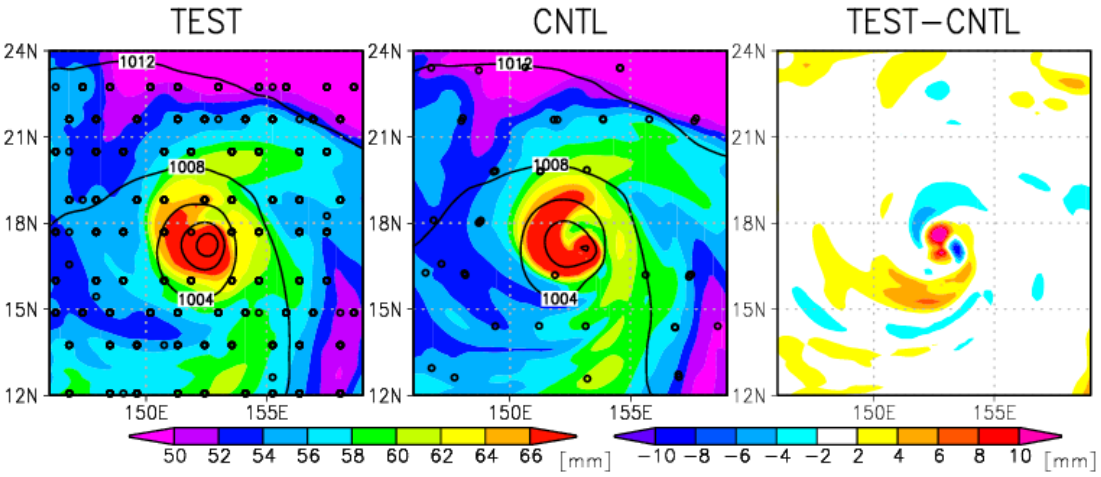

Figure 7. Assimilated microwave imager data (black dots) and analysis of total column water vapor amounts (shading) around the TC center at 06 UTC on 29 August with initial conditions. The left, center and right panels show TEST, CNTL and TEST-CNTL, respectively.

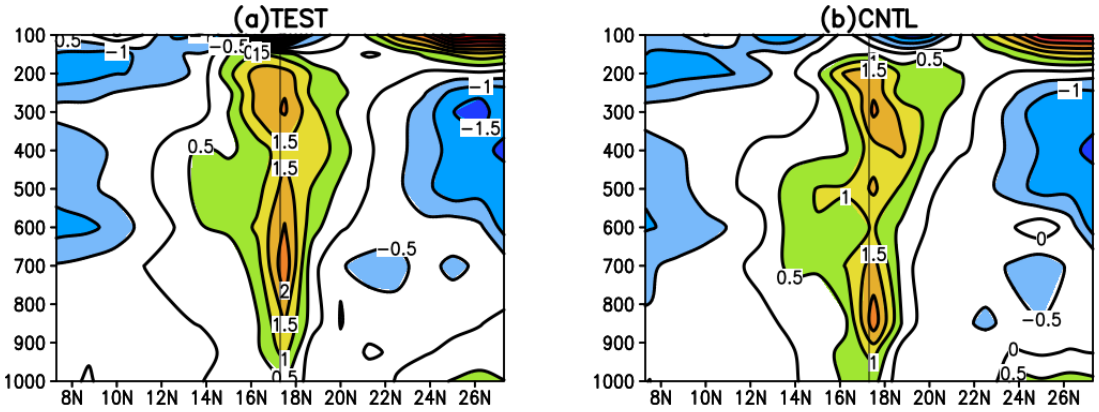

Figure 8. Temperature anomaly in the cross section at the TC center for (a) TEST and (b) CNTL

4. Summary

JMA began all-sky microwave radiance assimilation with outer-loop iteration for trajectory updates in the global NWP system on 11 December 2019. Improvement in the humidity, wind and temperature fields of FG departure statistics was observed in impact evaluation experiments for summer and winter 2018. RMSE values for geopotential height at 500 hPa and TC track forecasting were statistically improved as a result.

In relation to Typhoon Jebi (2018), track and intensity forecasting improvements were observed. Assimilation of microwave radiance data affected by cloud and precipitation around the TC center contributed to improved analysis of water vapor and temperature around the TC center.

References

Bauer, P., E. Moreau, F. Chevallier, and U. O'Keeffe, 2006: Multiple-scattering microwave radiative transfer for data assimilation applications. *Quart. J. Roy. Meteor. Soc.,* **132**, 1259–1281.

Geer, A. J., F. Baordo, N. Bormann, and S. J. English, 2014: All-sky assimilation of microwave humidity sounders. *ECMWF Tech. Memo.,* **741***, available from http://www.ecmwf.int.*

Geer, A. J., and P. Bauer, 2011: Observation errors in all-sky data assimilation. *Quart. J. Roy. Meteor. Soc.,* **137**, 2024–2037.

Kazumori, M., and T. Kadowaki, 2017: Development of an all-sky assimilation of microwave imager and sounder radiances for the Japan Meteorological Agency global numerical weather prediction system. *Tech. Proc. of 21st International TOVS Study Conference, Darmstadt, Germany 29 November – 5 December 2017.*

Okamoto, K., M. Kazumori, and H. Owada, 2005: The assimilation of ATOVS radiances in the JMA global analysis system. *J. Meteor. Soc. Japan*, **83**, 201–217.